ISSN 1674-1056
http://cpb.iphy.ac.cn
http://iopscience.iop.org/cpb
中国物理 B
Chinese Physics
中国物理 Chinese Physics B

Double superlattices structure for improving the performance of ultraviolet light-emitting diodes

Yan-Li Wang(王燕丽), Pei-Xian Li(李培咸), Sheng-Rui Xu(许晟瑞), Xiao-Wei Zhou(周小伟), Xin-Yu Zhang(张心禹), Si-Yu Jiang(姜思宇), Ru-Xue Huang(黄茹雪), Yang Liu(刘洋), Ya-Li Zi(訾亚丽), Jin-Xing Wu(吴金星), Yue Hao(郝跃)

Citation: Chin. Phys. B . 2019, 28(3): 038502. **doi:** 10.1088/1674-1056/28/3/038502
Journal homepage: http://cpb.iphy.ac.cn; http://iopscience.iop.org/cpb

What follows is a list of articles you may be interested in

Evaluation of current and temperature effects on optical performance of InGaAlP thin-film SMD LED mounted on different substrate packages

Muna E. Raypah, Mutharasu Devarajan, Fauziah Sulaiman
Chin. Phys. B . 2017, 26(7): 078503. **doi:** 10.1088/1674-1056/26/7/078503

Performance improvement of AlGaN-based deep ultraviolet light-emitting diodes with double electron blocking layers

Cheng Zhang(张诚), Hui-Qing Sun(孙慧卿), Xu-Na Li(李旭娜), Hao Sun(孙浩), Xuan-Cong Fan(范宣聪), Zhu-Ding Zhang(张柱定), Zhi-You Guo(郭志友)
Chin. Phys. B . 2016, 25(2): 028501. **doi:** 10.1088/1674-1056/25/2/028501

Large-scale SiO_2 photonic crystal for high efficiency GaN LEDs by nanospherical-lens lithography

Wu Kui, Wei Tong-Bo, Lan Ding, Zheng Hai-Yang, Wang Jun-Xi, Luo Yi, Li Jin-Min
Chin. Phys. B . 2014, 23(2): 028504. **doi:** 10.1088/1674-1056/23/2/028504

Performance improvement of GaN-based light-emitting diode with a p-InAlGaN hole injection layer

Yu Xiao-Peng, Fan Guang-Han, Ding Bin-Bin, Xiong Jian-Yong, Xiao Yao, Zhang Tao, Zheng Shu-Wen
Chin. Phys. B . 2014, 23(2): 028502. **doi:** 10.1088/1674-1056/23/2/028502

Color-converted remote phosphor prototype of multiwavelength excitable borosilicate glass for white light-emitting diodes

Tian Hua, Liu Ji-Wen, Qiu Kun, Song Jun, Wang Da-Jian
Chin. Phys. B . 2012, 21(9): 098504. **doi:** 10.1088/1674-1056/21/9/098504

Double superlattice structure for improving the performance of ultraviolet light-emitting diodes*

Yan-Li Wang(王燕丽)[1], Pei-Xian Li(李培咸)[1], Sheng-Rui Xu(许晟瑞)[2,†], Xiao-Wei Zhou(周小伟)[1,‡], Xin-Yu Zhang(张心禹)[1], Si-Yu Jiang(姜思宇)[1], Ru-Xue Huang(黄茹雪)[1], Yang Liu(刘洋)[1], Ya-Li Zi(訾亚丽)[1], Jin-Xing Wu(吴金星)[1], and Yue Hao(郝跃)[2]

[1] *The State Key Discipline Laboratory of Wide Band Gap Semiconductor Technology, School of Advanced Materials and Nanotechnology, Xidian University, Xi'an* 710071, *China*
[2] *The State Key Discipline Laboratory of Wide Band Gap Semiconductor Technology, School of Microelectronics, Xidian University, Xi'an* 710071, *China*

(Received 30 October 2018; revised manuscript received 19 December 2018; published online 23 January 2019)

The novel AlGaN-based ultraviolet light-emitting diodes (UV-LEDs) with double superlattice structure (DSL) are proposed and demonstrated by numerical simulation and experimental verification. The DSL consists of 30-period Mg modulation-doped p-AlGaN/u-GaN superlattice (SL) and 4-period p-AlGaN/p-GaN SL electron blocking layer, which are used to replace the p-type GaN layer and electron blocking layer of conventional UV-LEDs, respectively. Due to the special effects and interfacial stress, the AlGaN/GaN short-period superlattice can reduce the acceptor ionization energy of the p-type regions, thereby increasing the hole concentration. Meanwhile, the multi-barrier electron blocking layers are effective in suppressing electron leakage and improving hole injection. Experimental results show that the enhancements of 22.5% and 37.9% in the output power and external quantum efficiency at 120 mA appear in the device with double superlattice structure.

Keywords: light-emitting diodes (LEDs), electron blocking layer (EBL), superlattices

PACS: 85.60.Jb, 85.60.Bt, 73.40.Kp, 78.20.Bh **DOI:** 10.1088/1674-1056/28/3/038502

1. Introduction

Due to their non-toxic, no heat radiation, high switching speed, high energy, uniform illumination, and long service life, ultraviolet light-emitting diodes (UV-LEDs) have a wide variety of potential applications, such as UV curing, air purification, surface disinfection, sterilization of water, medical uses, and others.[1–5] However, there are still quite a few obstacles limiting the development of UV-LEDs photoelectric performance, such as the low doping concentration, the poor hole injection, and the severe electron leakage.[6–8] Numerous efforts have been made to solve these problems. On the one hand, since the periodic oscillation of the valence band can reduce the activation energy of the acceptor impurity, replacing the conventional p-type GaN layer with the Mg modulation-doped AlGaN/GaN superlattices (SL) could increase the hole concentration of the p-type GaN layer.[9,10] The introduction of a Mg-delta-doped hole injection layer has also been proposed to improve the hole doping efficiency of the p-type layer, thereby enhancing the light output power.[11,12] On the other hand, as many scholars have reported,[13–15] there are periodically varying electric fields in the short-period superlattice electronic barrier layer compared to the conventional electronic barrier layer, which can result in periodic variation of the energy band. And the conduction band barrier height is raised, suppressing the electron leakage into the p-type region, while the valence band barrier height is reduced, promoting the hole injection active region. Apart from this, the hole injection can also be supported by modifying the active region, which includes using the GaN/InGaN type last quantum barrier,[16] using the selective p-doped barriers,[17] reducing the quantum barrier thickness,[18] etc. In addition, a p-InAlGaN hole injection layer[19] and a hole accelerator[20] were also introduced for the sake of improving the hole injection, which could lead to the enhancement of internal quantum efficiency of the devices.

In our previous study, we proposed the short-period superlattice and analyzed the terahertz field in the short-period superlattice base on the energy dispersion relation.[21] Then, we also studied the effect of a multi-junction barrier electron blocking layer on the performance of UV-LEDs, and found that the output power of the devices is increased by 8.47%.[22,23] Although lots of methods have been presented to improve the photoelectric performance of UV-LEDs, the poor hole concentration and electron leakage problem still restrain their further development, especially under high current injection. For the above mentioned reasons, the novel AlGaN-based UV-LEDs with double superlattices structure (DSL) are proposed, which replace the p-GaN layer and electron block-

*Project supported by the National Key R&D Program of China (Grant Nos. 2016YFB0400800, 2016YFB0400801, and 2016YFB0400802), the National Natural Science Foundation of China (Grant No. 61634005), and the Fundamental Research Funds for the Central Universities, China (Grant No. JBZ171101).

†Corresponding author. E-mail: shengruixidian@126.com
‡Corresponding author. E-mail: xwzhou@mail.xidian.edu.cn

© 2019 Chinese Physical Society and IOP Publishing Ltd

ing layer (EBL) of conventional UV-LEDs with 30-period Mg modulation-doped p-AlGaN/u-GaN SL and 4-period p-AlGaN/p-GaN SL-EBL. The simulation results show that the DSL can increase the electron and hole concentrations in the active regions by modifying the energy band. In addition, the experimental results show that the output power and external quantum efficiency of the devices with DSL are increased by 22.5% and 37.9% at 120 mA, respectively.

2. Structures and parameters

As shown in Fig. 1(a), the conventional structure (sample A) was grown on a *c*-plane sapphire (0001) substrate by commercial metal organic chemical vapor deposition (MOCVD), with a 25 nm magnetron sputtering AlN buffer layer, a 2 μm undoped $Al_{0.02}Ga_{0.98}N$ layer, a 2.7 μm Si-doped n-type $Al_{0.02}Ga_{0.98}N$ layer (n-type dopant concentration $= 6 \times 10^{18}$ cm^{-3}), and the multiple quantum wells (MQWs) active regions consisting of eight 1.5 nm $In_{0.01}Ga_{0.99}N$ wells and nine 9 nm $Al_{0.08}Ga_{0.92}N$ barriers. On the top of the active regions, a 20 nm p-$Al_{0.2}Ga_{0.8}N$ EBL (p-type dopant concentration $= 6 \times 10^{19}$ cm^{-3}), a 150 nm p-GaN layer (p-type dopant concentration $= 6 \times 10^{19}$ cm^{-3}), and a 25 nm p$^+$-GaN (p-type dopant concentration $= 1 \times 10^{20}$ cm^{-3}) were grown. Sample B is identical to sample A except for the conventional p-GaN layer, which is replaced by 30-period 3 nm p-$Al_{0.16}Ga_{0.84}N$/2 nm u-GaN SL. While compared with sample A, sample C uses 30-period 3 nm p-$Al_{0.16}Ga_{0.84}N$/2 nm u-GaN SL and 4-period 3 nm p-$Al_{0.2}Ga_{0.8}N$/2 nm p-GaN SL as the p-GaN layer and p-EBL, respectively. Finally, the epitaxial wafers were etched into a mesa structure with sizes of 330.2 μm×304.8 μm by dry etching processes. Figure 1(b) shows the cross-sectional TEM image of sample C.

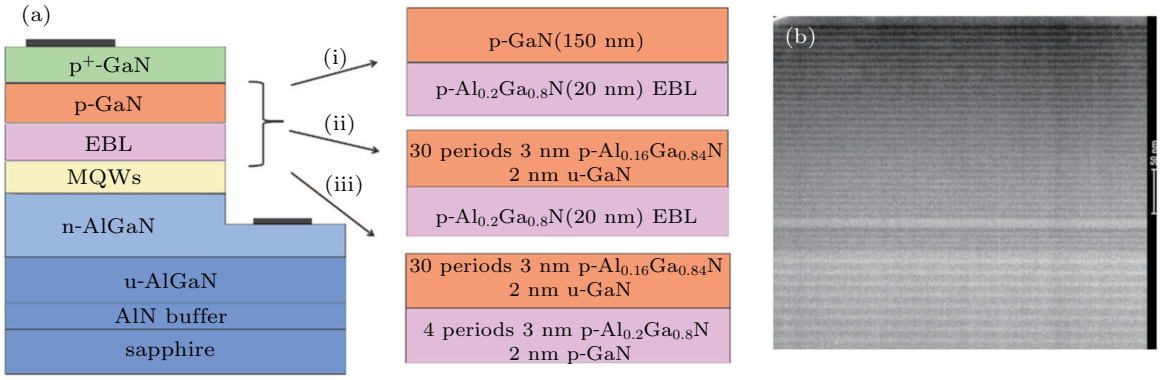


Fig. 1. (a) Schematic diagrams of (i) sample A, (ii) sample B, and (iii) sample C. (b) The cross-sectional TEM image of sample C.

The energy band diagrams, carrier concentration distribution maps, and radiative recombination rates of the UV-LEDs were numerically investigated with a finite element approach by the advanced physical model of semiconductor devices (APSYS), which was developed by Crosslight Software Inc. The operating temperature, Shockley–Read–Hall recombination lifetime, screening factor, and ionization energy of Mg were set to 300 K,[24] 100 ns, 50%,[25] and 0.2 eV,[26] respectively. The model used for the impurity activation was Poole–Frenkel model of incomplete ionization, which was important when the ionization energy was large.

3. Results and discussion

The conduction and valance band diagrams of samples A, B, and C at 120 mA are shown in Fig. 2. The effective potential barrier heights for electron (hole) of EBL are 356.9 meV, 365.7 meV, and 474.3 meV (121.7 meV, 98.8 meV, and 111.5 meV), respectively. Compared to sample A with a single electron barrier layer, sample C has multiple quantum barrier layers, which can cause multiple reflection effects of the electron wave function, thereby increasing the conduction band barrier height of the EBL by 117.4 meV. The increase in the effective potential height of sample C for electron effectively suppresses electron leakage to the p-type region.[27] For the valence band barrier of EBL, sample C has a lower value than sample A, which promotes hole injection into the active regions. However, as observed from Fig. 2(b), the lowest valence band effective barrier appears in sample B, which means that the introduction of polarization effect and interface stress can reduce the valence band barrier height of the single barrier layer. Moreover, due to the special energy band and polarization effect,[28] the AlGaN/GaN short-period superlattices in samples B and C generate periodic oscillation of the valence band, which will form a hole microstrip in the barrier layers.[29] The formation of the hole microstrip significantly reduces the ionization energy of the acceptor impurity. The valence band of the barrier layers is far from the Fermi level and the valence band of the well layers is close to the Fermi level, which cause the ionized holes to accumulate in the channel layers. And the farther the impurity level is away from the Fermi level, the lower the ionization energy of the acceptor impurity. The movement of holes generated by ionization above

the Fermi level breaks the ionization equilibrium, further promoting the ionization of the acceptor.[9]

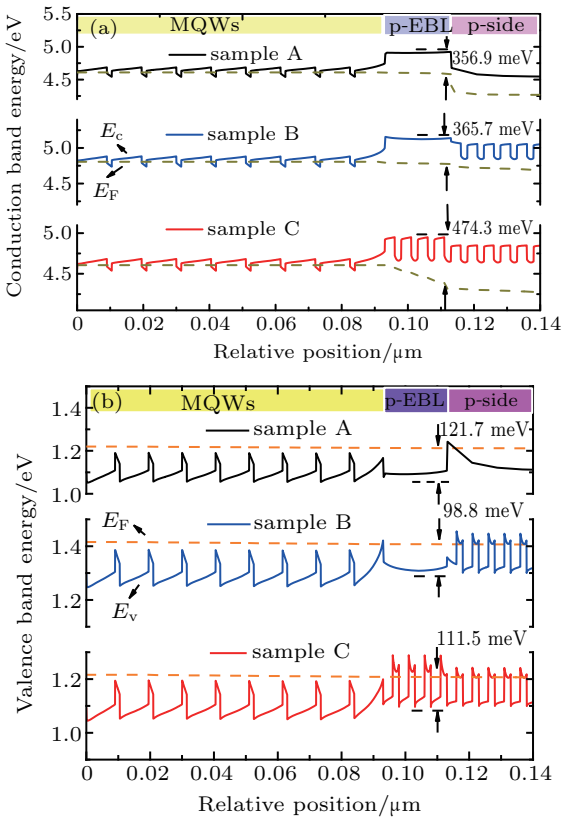


Fig. 2. Numerically simulated (a) conduction and (b) valance band diagrams of samples A, B, and C at 120 mA.

Figure 3 shows the electron and hole concentrations of the three samples at 120 mA. Due to the lower conduction band barrier height of the EBL of samples A and B, there are lower electron concentrations in the quantum wells and more leakage current in the p-type regions than that of sample C as shown in Fig. 3(a). Electrons leaked into the p-type regions are easily non-radiatively combined with holes, reducing the internal quantum efficiency of the devices.[30] The enlarged view in Fig. 3(b) shows that sample C has a larger hole concentration than samples A and B in the active regions and p-type layers, although sample B has the lowest valence band potential barrier of EBL. The phenomena above could be caused by two reasons. Firstly, the utilization of DSL can increase the ionization rate of Mg in the p-type layers by modifying the position of valance band edge relative to quasi-Fermi level, thereby improving the hole concentration, which is consistent with the conclusion in Fig. 2. Secondly, the multi-quantum barrier electron blocking layer in sample C can promote the hole injection active regions due to the quantum tunneling effect.[4] As found in Fig. 3(b), free holes in the superlattices are confined to the interfaces of the heterojunction and are separated into quasi-two-dimensional hole gas parallel to the interfaces. And because there are relatively few ionized impurities in the channel in which the hole is concentrated, the hole has a high mobility throughout the entire plane.[31] Figure 3(b) shows that the hole concentration of the AlGaN/GaN short-period superlattices is one order of magnitude higher than that of the conventional p-GaN layers.

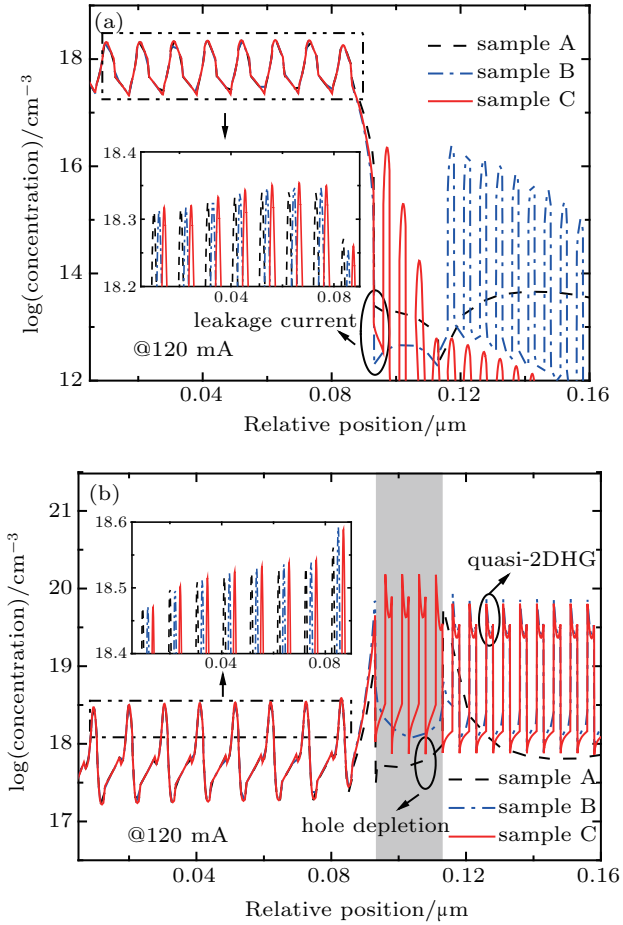


Fig. 3. Numerically simulated (a) electron and (b) hole concentration profiles of the three samples at 120 mA.

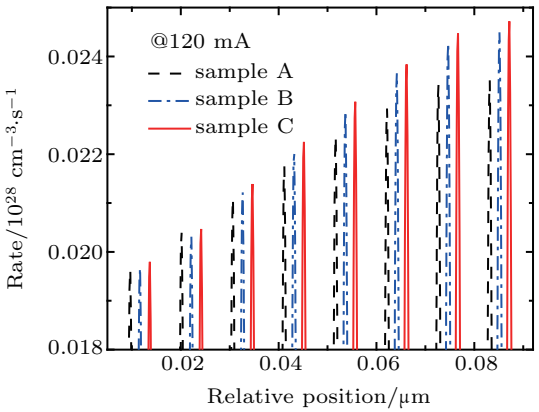


Fig. 4. Numerically simulated profile of the radiative recombination rate for the three samples at 120 mA.

The radiative recombination rates of the three samples at 120 mA are shown in Fig. 4. The horizontal positions of samples B and C have been shifted slightly for better observation. The figure shows that the radiative recombination rate

improves gradually from sample A to sample C. Sample C has the highest radiative recombination rate, which is the result of an increase in the concentration of electron and hole in the active regions.[32,33]

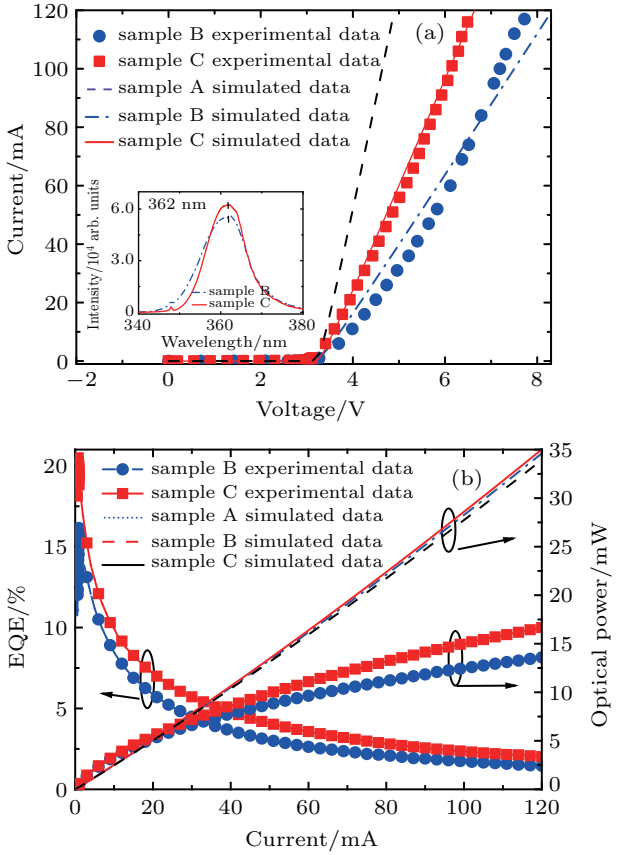


Fig. 5. (a) Measured *I*–*V* curves for samples B and C and simulated *I*–*V* curves for samples A, B, and C. Inset is the photoluminescence spectra of samples B and C. (b) Simulated optical output power of samples A, B, and C, and measured optical output power and external quantum efficiency of samples B and C.

Photoluminescence spectra of samples B and C at room temperature are shown in the inset of Fig. 5(a), for both of which the peak emission wavelength is approximately 362 nm. The emission characteristics of the samples were analyzed by the electroluminescent tester (No. LED617) produced by Weiming Corporation. The experimental *I*–*V* curves for samples B and C and simulated *I*–*V* curves for samples A, B, and C are displayed in Fig. 5(a). The simulated results of samples B and C are consistent with those obtained from experimental measurements, which verifies that the models used in this simulation match this study. Under 20 mA injection current, the forward voltages of samples B and C are 4.45 V and 3.91 V, respectively. The decrease in the forward voltage of 0.54 V is due to the use of DSL. The DSL can form discrete quasi-two-dimensional hole gas in the p-type layers, and the channel in which the hole is concentrated is less ionized, increasing the conductivity of the devices. However, it can be seen from the simulation results that the forward voltage of sample A is the smallest at 20 mA in comparison to those of samples B and C, because the short-period superlattices in samples B and C generate multiple quantum barriers along the growth direction to form a voltage drop, thereby increasing the series resistance. In response to the analysis of Figs. 2–4, the luminescence performance of devices is presented in Fig. 5(b). The simulated results show that the optical output powers of samples A, B, and C increase sequentially, which is the inferences shown above. The optical output powers of samples B and C driven at a current density of 20 mA are 5.22 mW and 5.51 mW, which correspond to the external quantum efficiency (EQE) of 5.86% and 7.14%, respectively. The improvement in optical performance of sample C with DSL is attributed to the higher hole concentration and less leakage current.[34,35] Note that, as the input power increases, the enhancement in the luminous power of sample C is more pronounced. For example, compared to sample B, an increase of 22.5% in the luminous power appears in sample C at 120 mA. This may be because the effect of sample C on suppressing leakage is even more obvious as the input power increases. And the EQE of sample C at 120 mA is 37.9% higher than that of sample B, indicating that the DSL reduces the droop effect of the devices at high power current.

4. Conclusion

We propose the double superlattice structure consisting of 30-period Mg modulation-doped p-AlGaN/u-GaN SL and 4-period p-AlGaN/p-GaN SL-EBL. Based on simulation analysis and experimental verification, the DSL has been proven to be very useful in suppressing electron leakage, increasing hole concentration, and improving hole injection. Therefore, the enhancements of 22.5% and 37.9% in the output power and external quantum efficiency at 120 mA appear in the device with double superlattice structure.

References

[1] Yu H P, Li S B, Zhang P, Wu S H, Wei X B, Wu Z M and Chen Z 2014 *Chin. Phys. Lett.* **31** 108502
[2] Qin P, Song W D, Hu W X, Zhang Y W, Zhang C Z, Wang R P, Zhao L L, Xia C, Yuan S Y, Yin Y A, Li S T and Su S C 2016 *Chin. Phys. B* **25** 088505
[3] Dai F, Zheng X F, Li P X, Hou X H, Wang Y Z, Cao Y R, Ma X H and Hao Y 2016 *Chin. Phys. Lett.* **33** 117301
[4] Li Y, Chen S C, Tian W, Wu Z H, Fang Y Y, Dai J N and Chen C Q 2013 *IEEE Photon. J.* **5** 8200309
[5] Du X Z, Lu H, Chen D J, Xiu X Q, Zhang R and Zheng Y D 2010 *Chin. Phys. Lett.* **27** 088105
[6] Zhang Z H, Zhang Y H, Bi W G, Geng C, Xu S, Demir H V and Sun X W 2016 *Appl. Phys. Lett.* **108** 133502
[7] Schubert E F, Grieshaber W and Goepfert I D 1996 *Appl. Phys. Lett.* **69** 3737
[8] Chen S C, Li Y, Tian W, Zhang M, Li S L, Wu Z H, Fang Y Y, Dai J N and Chen C Q 2015 *Appl. Phys. A* **118** 1357
[9] Kozodoy P, Smorchkova Y P, Hansen M, Xing H L, DenBarrs S P, Mishra U K, Saxier A W, Perrin R and Mitchel W C 1999 *Appl. Phys. Lett.* **75** 2444
[10] John S, Vladimir P, Lian C X, Xing H L and Debdeep J 2010 *Science* **327** 60

[11] Xian Y L, Huang S J, Zheng Z Y, Fan B F, Chen Z M, Wu Z S, Wang G, Zhang B J and Jiang H 2013 *J. Disp. Technol.* **9** 255

[12] Li T, Wang H B, Liu J P, Niu N H, Zhang N G, Xing Y H, Han J, Liu Y, Gao G and Shen G D 2007 *Acta Phys. Sin.* **56** 1036 (in Chinese)

[13] Tong J H, Zhao B J, Wang X F, Chen X, Ren Z W, Li D W, Zhuo X J, Zhang J, Yi H X and Li S T 2013 *Chin. Phys. B* **22** 068505

[14] Gong C C, Fan G H, Zhang Y Y, Xu Y Q, Liu X P, Zheng S W, Yao G R and Zhou D T 2012 *Chin. Phys. B* **21** 068505

[15] Cai J X, Sun H Q, Zheng H, Zhang P J and Guo Z Y 2014 *Chin. Phys. B* **23** 058502

[16] Shi Q, Li L P, Zhang Y H, Zhang Z H and Bi W G 2017 *Acta Phys. Sin.* **66** 58501 (in Chinese)

[17] Chen J, Fan G H and Zhang Y Y 2012 *Acta Phys. Sin.* **61** 088502 (in Chinese)

[18] Ju Z G, Liu W, Zhang Z H, Tan S T, Ji Y, Kyaw Z B, Zhang X L, Lu S P, Zhang Y P, Zhu B B, Hasanov N, Sun X W and Demir H V 2013 *Appl. Phys. Lett.* **102** 243504

[19] Yu X P, Fan G H, Ding B B, Xiong J Y, Xiao Y, Zhang T and Zheng S W 2014 *Chin. Phys. B* **23** 028502

[20] Zhang Z H, Zhang Y H, Bi W G, Geng C, Xu S, Demir H V and Sun X W 2016 *Appl. Phys. Lett.* **108** 151105

[21] Chen J F and Hao Y 2009 *Chin. Phys. B* **18** 5451

[22] Huang Y, Li P X, Yang Z, Hao Y and Wang X B 2014 *Sci. Chin. Phys. Mech. Astron.* **57** 887

[23] Huang Y, Li P X, Bai J C and Wang X B 2014 *Electron. Sci. Tech.* **27** 184

[24] Wu L J, Li S T, Liu C, Wang H L, Lu T P, Zhang K, Xiao G W, Zhou Y L, Zheng S W, Yin Y A and Yang X D 2012 *Chin. Phys. B* **21** 068506

[25] Liu C, Ren Z W, Chen X, Zhao B J, Wang X F, Yin Y A and Li S T 2013 *Chin. Phys. B* **22** 058502

[26] Waldron E L, Li Y L, Schubert E F, Graff J W and Sheu J K 2003 *Appl. Phys. Lett.* **83** 4975

[27] Shi Q, Li L P, Zhang Y H, Zhang Z H and Bi W G 2017 *Acta Phys. Sin.* **66** 158501 (in Chinese)

[28] Tian W, Yan W Y, Xiong H, Dai J N, Fang Y Y, Wu Z H, Yu C H and Chen C Q 2013 *Chin. Phys. B* **22** 057302

[29] Xia J B and Zhu B F 1995 *Semiconductor Superlattice Physics* (Shanghai: Science and Technology Press) p. 6

[30] Shih Y H, Chang J Y, Sheu J K, KuoY K, Chen F M, Lee M L and Lai W C 2016 *IEEE Trans. Electron. Dev.* **63** 1141

[31] Kumakura K, Kobayashi N and Makimoto T 2000 *Jpn. J. Appl. Phys.* **39** 2428

[32] Ding B B, Zhao F, Song J J, Xiong J Y, Zheng S W, Zhang Y Y, Xu Y Q, Zhou D T, Yu X P, Zhang H X, Zhang T and Fan G H 2013 *Chin. Phys. B* **22** 088503

[33] Chen J, Fan G H and Zhang Y Y 2012 *Acta Phys. Sin.* **61** 038502 (in Chinese)

[34] Zhang M, Li Y, Chen S C, Tian Wu, Xu J T, Li X Y, Wu Z H, Fang Y Y, Dai J N and Chen C Q 2014 *Superlattices Microstruct.* **75** 63

[35] Zhang Y Y and Fan G H 2011 *Chin. Phys. B* **20** 048502